Uncertainty in the Maximum Principal Stress Estimated from Hydraulic Fracturing Measurements Due to the Presence of the Induced Fracture

Jonny Rutqvist and Chin-Fu Tsang
Earth Sciences Division
Lawrence Berkeley National Laboratory
Berkeley, CA 947 20 USA

Ove Stephansson
Royal Institute of Technology
Division of Engineering Geology
S-100 44 Stockholm, Sweden

International Journal Rock Mechanics and Mining Sciences
Vol. 37, pp. 107-120, 2000

Abstract

The classical theory for hydraulic fracturing stress measurements assumes an ideal case with a linear elastic, homogenous, and isotropic medium; and a fracture that reopens distinctly when the minimum tangential borehole stress is exceeded. The induced fracture disturbs this ideal picture in several aspects, which are important for the evaluation of the maximum horizontal principal stress using the fracture reopening pressure. This disturbance can be attributed to the fracture normal stiffness and the initial hydraulic fracture permeability. In this paper, the hydraulic fracturing reopening test is studied by coupled hydromechanical modeling that takes into account an induced fracture that is incompletely closed. The result shows that with realistic equipment compliance, the apparent fracture reopening evaluated from the well-pressure is close to the magnitude of the minimum horizontal principal stress with little or no correlation to the maximum horizontal principal stress. This observation suggests that determination of maximum principal stress by hydraulic fracturing using the reopening pressure is very uncertain.

Introduction

Hydraulic fracturing is a common technique for stress measurements in deep boreholes. This technique involves measuring the stress normal across a fracture plane from the fluid pressure supporting it during a hydraulic pressurization. Hydraulic pressurization is conducted with specialized equipment for high-pressure injection, and includes packers to seal off a section of a borehole and a hydraulic line connected to the ground surface (Figure 1). During hydraulic fracturing, the borehole is pressurized by fluid injection with a pump located on the ground surface. The pump-injection flow, Q_w, is measured on the ground, but the well-pressure, P_w, may be measured down hole. Between the pump and the downhole packer, there may be several hundreds of meters of water pipes or hydraulic hoses, which expand upon pressurization, providing a well storage, S_w. Because of temporary water storage in the expanding hydraulic line, the flow rate into the fracture may be considerably different from the actual pump-injection rate.

The classical hydro-fracturing stress measurement technique aims to determine both the minimum and maximum compressive principal horizontal stress (also denoted minimum and maximum horizontal stress). A vertical hydraulic fracture is induced within a vertical borehole perpendicular to the minimum horizontal stress (Figure 2). The fracture is induced and propagated by injecting water at a constant flow rate. During the injection, the well-pressure increases with time due to the storage effects in the hydraulic hose, until the borehole wall breaks and fluid is lost into the rock formation (Step 2 in Figure 2). At this moment, the well-pressure sharply decreases due to unstable propagation of the fracture. The injection is then stopped and the hydraulic line shut-in by closing a shut-in valve, and the shut-in pressure, P_s, is determined to evaluate the minimum horizontal stress σ_h (Step 3 in Figure 2). After shut-in, the pressure continues to decrease due to fluid leakage in to the surrounding rock. A few minutes after shut-in, the valve is opened to restore the ambient pressure in the fracture before a reopening test is commenced.

The reopening test is conducted by injecting fluid at the same rate as the previous fracturing cycle. Again, the well-pressure increases with time due to the storage of water

in the hydraulic hose, as long as the fracture is "closed." Later, when the pressure is high enough to reopen the fracture, the well-pressure stabilizes and then drops slightly, due to loss of water into the fracture (Step 4 in Figure 2). The pressure at the moment when the pressure versus time curve deviates from its sub-linear increasing trend can be interpreted as the fracture reopening pressure. After a few minutes of injection, the pump is again stopped and the hydraulic hose to the test interval kept shut-in.

The minimum horizontal stress, σ_h is determined from the shut-in pressure; the maximum horizontal stress, σ_H, may be evaluated using Bredehoeft's [1] equation:

$$\sigma_H = 3\sigma_h - P_r - P_0 \quad (1)$$

where P_r is the reopening pressure and P_0 is the pore pressure in the fracture. This equation is derived from the Kirsch solution for a circular hole subjected to an internal pressure in an isotropic, homogeneous and, linear elastic medium. It is assumed that the reopening occurs when the fluid pressure applied on the borehole wall is high enough to cancel out the minimum tangential stress (σ_θ^{min} in Figure 2) at the borehole wall, resulting from the two remote horizontal stresses:

$$\sigma_\theta^{min} = 3\sigma_h - \sigma_H \quad (2)$$

In the field, it has been shown that the reopening pressure depends on the injection flow rate [2]. This dependency indicates that the fluid is penetrating the fracture and opens it by internal pressure inside the fracture. If fluid is penetrating the fracture, the use of Equation (1) may give a poor estimate of the maximum horizonatal stress and an alternative equation should be used [3].

In a recent study, Rutqvist and coworkers [4] conducted pulse injection tests on hydraulic fractures in granitic rocks, at depths between 297 and 697 meters. The tests showed that the fractures were incompletely closed, with a hydraulic aperture of 3 to 5 μm near the borehole and 6 to 15 μm away from the borehole. The study also indicated that the hydraulic fractures had similar properties to tensile fractures induced in core samples [5], with a normal stiffness of 2000 GPa/m or less. Based on these fracture properties, Rutqvist and Stephansson [6] performed coupled numerical modeling of reopening tests on a vertical fracture in an isotropic stress field of 10 MPa. They performed a parameter variation and concluded that the fracture reopening evaluated from the well-pressure depends on the properties of both the induced fracture and the hydraulic fracturing equipment. Most important parameters for determining the reopening pressure are the fracture normal stiffness, residual hydraulic fracture aperture, and injection rate.

This paper studies the effect of the induced fracture on determining the maximum horizontal stress when using the reopening pressure. Reopening tests are simulated using coupled hydromechanical modeling, with consideration of fracture normal stiffness and initial hydraulic fracture permeability. It aims to find the relation between the reopening pressure and the remote stress field, considering realistic equipment and fracture properties.

Possible uncertainties due to the induced fracture

The sources of uncertainty due to the induced fracture can be attributed to the fracture normal stiffness and initial hydraulic aperture. There are three possible uncertainties:

(1) In the ideal case, assumed in the classical hydraulic fracturing theory, the fracture has the same mechanical properties as the surrounding rock except that it has no tensile strength. Thus, it is assumed that the rock is linear elastic, homogenous, and isotropic. If, on the other hand, the fracture is mechanically softer than the surrounding rock matrix, the stress tends to be smeared out along the fracture, reducing the stress concentration at the borehole wall. In such case, the minimum tangential stress can no longer be calculated from the solution in Equation (2), and therefore an error is introduced in the estimate of maximum horizontal stress when using Equation (1).

(2) In the ideal case, the fracture is initially completely closed and begins to open at the moment the effective normal stress across the fracture is equal to zero. However, it is known from numerous laboratory tests that rock fractures open gradually as a function of the effective stress, and that they can conduct water in voids between surface contact points. Thus, during a reopening test, the fracture may therefore open gradually as a function of time, and a distinct reopening pressure is difficult to detect.

(3) In the ideal case, no fluid is penetrating the fracture until fracture reopening. If, on the other hand, the fracture is conducting water in its incompletely closed position (resting on its surface asperities), the evaluation of the maximum horizontal stress will be affected (Figure 3). If the fracture is slightly conductive, the pressure may only partially penetrate and the pressure inside the fracture at the borehole wall is equal to the well-pressure (Figure 3b). In such case, P_0 in Equation (1) can be replaced with P_r to obtain [7]:

$$\sigma_H = 3\sigma_h - 2P_r \quad (3)$$

In the extreme case, with a more conductive fracture, the fluid pressure may completely penetrate to the crack tip, forming a uniform pressure along the fracture (Figure 3c). This implies that the reopening is dominated by the total force formed by the fluid pressure on the fracture surfaces, and the reopening pressure would be equal to the minimum horizontal stress:

$$\sigma_h = P_r \quad (4)$$

In this case it is not possible to determine the maximum horizontal stress because the pressure response would not show any effect of the tangential borehole stress.

In summary, the validity of Equations 1, 3, or 4 depends on whether fracture reopening is due to the fluid pressure on the borehole wall or whether opening takes place as a result of the fluid pressure inside the fracture. This issue is investigated by the coupled numerical modeling in the next section.

Coupled numerical modeling of reopening tests

The reopening tests are modeled with the coupled hydromechanical finite element program ROCMAS [8] and includes coupled stress and fluid flow in both the fracture and the surrounding rock matrix. The modeling is conducted in a horizontal section through the borehole and the fracture, as shown in Figure 1.

Model geometry

Figure 4 presents the model geometry and mechanical boundary conditions. It consists of 1200 elements, including special joint elements for the hydraulic fracture. The borehole is 76 mm in diameter and the size of the model is 7 by 7 meters. At the borehole wall, the

fluid pressure and the total stress normal to the wall surface are equal to the current well-pressure.

Material properties

Table 1 presents the material properties for modeling the reopening tests with the ROCMAS code. These include appropriate coupling parameters for the stress and fluid flow interaction based on Biot's generalized effective stress law [9]. Most parameters have been measured either by laboratory experiments or by hydraulic field testing on fractures in competent granitic rock [4]. Of the all the parameters given in Table 1, the fluid and fracture properties are most important. The properties of the low permeable rock matrix are not important for the results in this study. The fracture is modeled with nonlinear normal stress versus normal displacement relation according to Goodman [10] or Bandis [11]. In this study, a mechanical fracture aperture b_m is defined as being equal to the current maximum normal closure, which according to Goodman's model is related to the effective normal stress, σ'_n, as:

$$\sigma'_n = \frac{A_i}{b_m} \tag{5}$$

where A_i is a constant defined as:

$$A_i = \sigma'_{ni} \cdot b_{mi} \tag{6}$$

where σ'_{ni} and b_{mi} are the effective normal stress and mechanical aperture, respectively, at an initial or reference state. It can be shown that Bandis' fracture normal closure model is similar to Goodman's, but the curve is displaced along the stress axis (Figure 5). Bandis' joint model can therefore be written in an analogous way to Equation (5) as:

$$\sigma'_n = \frac{A_i}{b_m} + \sigma'_{n0} \tag{7}$$

where σ'_{n0} is defined and related to the conventional Bandis' parameters (k_{n0} and b_{m0}) [11], as depicted in Figure 5. However, in this study, Bandis' normal closure curve is completely defined by the two parameters A_i and σ'_{n0}.

The normal stiffness, k_n, of the fracture is:

$$k_n = \frac{\partial \sigma'_n}{\partial b_m} = \frac{\sigma'_n + \sigma'_{n0}}{b_m} \tag{8}$$

The effective stress in the fracture is related to the total stress, σ_n, and the fluid pressure, p, according to:

$$\sigma'_n = \sigma_n - \alpha \cdot p \tag{9}$$

where α is Biot's effective stress parameter [9].

The hydraulic aperture b_h is defined from fracture transmissivity T through the "cubic law" [12]:

$$b_h = \sqrt{\frac{T 12 \mu_f}{\rho_f g}} \tag{10}$$

where μ_f and ρ_f are dynamic viscosity and density of the fluid, and g is the gravitational acceleration. The hydraulic aperture is coupled to the mechanical aperture according to:

$$b_h = b_{hr} + f \cdot b_m \quad (11)$$

where b_{hr} is the residual hydraulic aperture when the fracture is mechanically closed and f is a factor that compensates for the deviation of flow in a natural rough fracture from the ideal case of parallel-plate-type fracture surfaces [12].

Modeling of stress redistribution due to the induced fracture

This calculation aims to study the changes that occur in the stress field as a result of the hydraulic fracturing during the first pressurization cycle (Figure 2). In the modeling, the fracture is opened from a perfectly closed stage and thereafter closed again to an equilibrium condition. However, the fracture does not close completely but will be kept slightly open, resting on its surface asperities. The effect of the surface asperities is simulated though the joint model in Equations (7) to (11), resulting in a fracture normal stiffness and hydraulic aperture based on the current normal stress across the fracture.

Figure 6 presents the results of one simulation where the remote stress is isotropic at 10 MPa, and the fluid pressure is zero. The minimum tangential stress, $\sigma_{\theta min}$, before fracturing is about 20 MPa, which agrees with the analytical solution in Equation (2). After fracturing, on the other hand, $\sigma_{\theta min}$ is about 17 MPa, which is less than the theoretical value of 20 MPa. Fracture normal stiffness is about 1000 GPa/m at the borehole wall and 600 GPa/m at a distance of 0.5 meters into the fracture. Fracture hydraulic aperture is about 4 μm and 7 μm at the same respective locations.

Figure 7 presents the borehole wall stress concentration factor ($\sigma_{\theta min}/\sigma_h$) versus minimum horizontal stress for different horizontal stress factors (σ_H/σ_h). In the example in Figure 6, the principal stress factor is 1 and should in the ideal case give a wall stress concentration factor of 2 according to Equation (2). However, due to the influence of the fracture normal stiffness, the stress concentration factor becomes 1.7 (Figure 8 at 10 MPa minimum horizontal stress). At higher stress, the fracture normal stiffness increases, and therefore the borehole wall stress concentration factor approaches the solution for the ideal case.

Two cases of anisotropic stress field are also presented in Figure 7. When the maximum horizontal stress magnitude is 3 times the minimum horizontal stress, Equation (2) predicts that $\sigma_{\theta min}$ would be zero. However, the modeling including the fracture shows that it is very difficult to attain a situation with zero tangential borehole stress. As shown in Figure 7, there is always a significant error compared to the ideal case when the maximum horizontal stress is 3 times minimum horizontal stress. In general, the disturbance of the induced fracture increases relative to the ideal case, at lower stress magnitudes. At very low stress, in the order of a few MPa, the resulting minimum tangential stress of all three cases of remote stress factor converges to the same value.

Modeling of fracture reopening tests

This calculation aims to find the relation between minimum and maximum horizontal stress and the reopening pressure. Hydraulic fracturing reopening tests are simulated by injecting fluid at a constant rate. The well storage capacity S_w (Figure 1) is assumed to be $3.1 \cdot 10^{-10}$ m^3/Pa according to an existing hydraulic fracturing equipment [13]. The initial

fracture length is 1 meter, according to field measurements by Rutqvist *et al*. [4]. This is not a critical parameter, since a sensitivity study showed that the reopening pressure is not dependent on the fracture length for fractures longer than 0.5 meters [6]. The reopening tests are simulated at two different magnitudes of minimum horizontal stress. First at a moderate rock stress of 10 MPa, and then at a high rock stress of 50 MPa, and in each case the horizontal stress factor (σ_H/σ_h) is varied between 1 and 3. Finally, one case of simulation is conducted with an extremely small well storage capacity to demonstrate the importance of the equipment compliance.

Reopening at moderate rock stress

In this case, the minimum horizontal stress is set to 10 MPa and the maximum horizontal stress is varied between 10 and 30 MPa. This stress magnitude could represent a measurement conducted at a few hundred meters depth in granitic rocks. The pump-injection rate is set to 6 liters/minute to achieve the peak pressure in about 30 seconds.

Figure 8 presents modeling results of well-pressure and flow into the induced fracture as a function of time. The figure compares the well-pressure response with a fracture to the well-pressure response without a fracture. The modeling without a fracture represents the first pressurization cycle before break-down, and the modeling with a fracture corresponds to the second pressurization cycle (Figure 2). In Figure 8, there is no visible difference in the results until the pressure has reached about 11 MPa. At this time, the flow rate into the fracture is about 0.5 liter/minute, which is significant compared to the pump-injection flow rate. Because a significant amount of fluid is lost from the well into the fracture, the well-pressure deviated from its earlier linear and well-storage-dominated response. At peak-pressure, the fracture has apparently opened so much that the flow into the fracture now is equal to the pump-injection rate. Thus, the same amount of water is pumped into the well as lost by leakage into the fracture and, hence, the well-pressure no longer increases. After peak pressure, the flow into the fracture is larger than the injection rate because some of the water stored in the expanded water houses is released and the well-pressure decreases slightly.

A startling and very important observation from Figure 8 is that both the well-pressure and fracture flow appears to be independent of the maximum horizontal stress. Thus, the reopening pressure is 11 MPa in both cases with no correlation to the maximum horizontal stress.

Figure 9 presents the pressure, hydraulic aperture, and effective normal stress along the fracture at four different times, and helps to explain why the well-pressure is independent of the maximum horizontal stress. The figure shows that the fracture opening is gradual as a function of time starting at the borehole wall. Already after 10 seconds, fluid has penetrated far into the fracture and forced it to open (Figure 9a and b). At this time, the hydraulic aperture is small and the flow rate into the fracture is still insignificant in comparison to the pump-injection rate. However, even if the flow rate into the fracture is very small, the fluid pressure penetrates the fracture very fast and initiates fracture opening. Thus, the actual fracture opening starts much earlier than the reopening pressure

seen in the well-pressure response at 20 seconds of Figure 8. The reopening pressure in Figure 8 can therefore be denoted an apparent reopening pressure.

At the time of the apparent reopening pressure (20 seconds), the pressure has penetrated 1 meter to the outer edge of the fracture (Figure 9a). As was observed in Figure 8, the flow rate into the fracture is now significant in comparison to the injection rate, and therefore the well-pressure deviates from the earlier linear trend. At this time, the difference in fracture aperture at the borehole depending on the maximum horizontal stress is relatively small (20 seconds, Figure 9b). This small and very near-field effect of the maximum horizontal stress is insignificant to the overall pressure and fracture opening response. Instead, the well-pressure and the fracture opening is dictated by the total force formed by the fluid pressure inside the fracture, and with little or no influence of the borehole wall pressure. After attaining the apparent reopening pressure, the fracture opening is accelerated due to the reduction of fracture normal stiffness when the effective stress normal to the fracture approaches zero (Figure 9c).

Reopening at high rock stress

The minimum horizontal stress is increased to 50 MPa, which could correspond to a measurement conducted below 1,000 meters depth. The horizontal stress factor is 1 and 3 giving a maximum horizontal stress as high as 150 MPa, which may be unrealistic. The remaining model parameters are the same as in the previous moderate stress case, except that the pump-injection rate has been increased from 6 to 40 liters/minute in order to reach the peak pressure within 30 seconds. According to Figure 7, the wall stress concentration is now much closer to the ideal case. The increased stress level also implies that the fracture now is much more compressed, with a high normal stiffness in the order of 30 000 GPa/m and a small initial aperture of about 1 μm.

Despite a large variation of the maximum horizontal stress between 50 to 150 MPa, the well-pressure during the entire reopening test is almost identical (Figure 10). The apparent reopening pressure is about 60 MPa, with a slightly lower value when the maximum horizontal stress is higher. Thus, there is a small discernible difference in the pressure response, because the flow rate into the fracture increases slightly earlier when the maximum horizontal stress is higher.

Figure 11 shows that the fracture response is similar to the moderate stress case (Figure 9), with gradual fracture opening starting at the well-bore at a much smaller pressure than the apparent reopening pressure. In this case, however, the fracture is opened in a more distinct fashion, with a sharper opening front propagating outwards. There is also considerable dependency on maximum horizontal stress in the fracture aperture and propagation of the fluid pressure. When the maximum horizontal stress is 150 MPa, the fluid pressure penetrates the fracture earlier, resulting in a larger aperture at the same time. However, it is interesting to note that, despite considerable differences in pressure response inside the fracture, the pressure at the well-bore is not affected significantly. Furthermore, at reopening (t = 20 seconds), the pressure gradient near the well-bore is very small. This low gradient indicates that the viscous effect at the fracture inlet is small,

hence, the flow into the fracture is dependent on available storage rather than hydraulic permeability. This observation suggests that the apparent reopening pressure reflects a change in the total storage of the system, due to a change in the fracture stiffness during the fracture opening and gradual loss of surface asperity contacts.

Reopening at high rock stress and very small well storage

In another numerical simulation, the minimum horizontal stress is kept to 50 MPa, but the well-bore storage S_w is reduced from $3.1 \cdot 10^{-10}$ m^3/Pa to $1.0 \cdot 10^{-12}$ m^3/Pa. This represents the storage produced by the compressibility of water of the volume in a half-a-meter long packed off section of the borehole. This is a very low well-bore storage that theoretically could be obtained only if the pump were placed directly above the packers, and there were negligible mechanical compliance of the packer during pressurization. The flow rate has to be as small as 0.1 liters/minute in order to reach the peak pressure at about 30 seconds.

In this case, the influence of the maximum horizontal stress is clear in both the well-pressure and the fracture flow (Figure 12). When the maximum horizontal stress is 150 MPa, the fracture flow increases earlier, resulting in an apparent reopening pressure of about 30 MPa. When the maximum horizontal stress is 50 MPa, the apparent reopening pressure is about 40 MPa. These interpretations of the reopening pressure are though very subjective and depends on the resolution of the graph.

The clear effect of the maximum horizontal stress in this case can be explained with the low well storage and the fracture response presented in Figure 13. When the maximum horizontal stress is 150 MPa, the fracture is initially much more open near the well-bore, where it has a much smaller fracture normal stiffness. The water, therefore, penetrates the fracture easily and the fracture has opened considerably at 10 seconds. Apparently the stiffness of the fracture at the borehole wall is low and thus the fracture volume increases sufficiently fast to affect the well-bore pressure. When the maximum horizontal stress is 50 MPa, on the other hand, the aperture at the well-bore contact is much smaller and the fluid cannot easily penetrate, and at 10 seconds the fracture has not opened to any considerable degree (Figure 13b). The small aperture at the well-bore contact is here working as a bottleneck, resulting in viscous resistance to flow (which can be seen as a higher pressure gradient in Figure 13a). It is important to note that the same “bottleneck effect” can be seen in Figure 11a at 10 seconds. However, in that case, the well-pressure is not affected since it is still dominated by the larger well storage.

This modeling case demonstrates that the fracture response in the borehole wall can be sensed in a reopening test, if the well-bore storage is very low. However, the flow rate is so small that the fracture only opens about 5 μm at the apparent reopening pressure. This lack of response implies that the fracture is far from completely open, and that the effective normal stress is still high across the fracture.

Summary and interpretation of modeling results

The modeling results indicate that the apparent reopening pressure reflects a change in the total compliance of the injection system. The system compliance is here defined as

$\Delta V/\Delta P$, where ΔV is the water volume change due to the pressure change ΔP. For the equipment, this is equal to the storage capacity, S_w. For the fracture, ΔP is the well-pressure and ΔV is the accompanying fracture volume increase. The fracture compliance is strongly related to the fracture normal stiffness and may also depend on the stiffness of the surrounding rock and fracture length. During the early part of the test, the flow rate into the fracture is very small compared to the injection flow rate, and therefore can not be detected in well-pressure response. The fluid pressure can, however, propagate into the fracture in a matter of seconds, causing a gradual fracture opening with time. When the effective normal stress and normal stiffness decreases, the fracture becomes more compliant and the fracture opening is accelerated. This causes a dramatic increase in fracture flow, and the well-pressure deviates from its earlier well-storage-dominated response. This point defines the apparent reopening pressure.

The modeling of the reopening tests shows that, assuming a reasonable well-bore storage, the maximum horizontal stress has very little effect on the well-pressure. In these cases, the apparent reopening pressure was slightly above the stress perpendicular across the fracture, which is the minimum horizontal stress (Table 2). Thus, the results indicate that we have the situation illustrated in Figure 3c, and that Equation (4) most accurately defines the reopening pressure.

Assuming a very small well-bore storage, the well-pressure response becomes dependent on the maximum horizontal stress. This is because the equipment compliance and the injection rate are so small that the very-near-borehole fracture respons can be detected in the well-pressure response. An anistropic stress field results in a smaller minimum tangential borehole stress, which in turn results in a lower fracture normal stiffness at the borehole contact. Therefore, in an anisotropic stress field, the total system compliance will change earlier and result in a lower apparent reopening pressure. Although there is a clear dependency on the maximum horizontal stress in this case, there is no good correlation to either of Equations (1) or (3). When the well-bore storage is small, the reopening pressure is lower than the stress perpendicular to the fracture plane, but Equation (4) is still the most accurate (Table 2).

Discussion

Our modeling shows that in most practical situations the apparent reopening pressure will be similar to the minimum horizontal stress, which also is about the same magnitude as the shut-in pressure. The reopening pressure may vary slightly depending on the evaluation method and on the compliance of the test equipment. In general, equipment with a larger volumetric expansion during pressurization will yield a higher reopening pressure.

Our results support findings by Cheung and Haimson [14] and Lee and Haimson [15]. They found, in a series of laboratory and field experiments, that the reopening pressure appeared to be very nearly the estimate of the shut-in pressure. They also made a literature review, studying 15 randomly selected hydro-fracturing sites worldwide in different rocks, and found that the difference between the reopening and shut-in pressure at those sites never exceeded 25%.

Our results also support theoretical studies by Morita *et al.* [16], Guo *et al.* [17] and Ratigan [18]. They aimed to study the secondary break-down pressure during fracture reopening using linear elastic fracture mechanics. One main conclusion from these studies is that the secondary break-down pressure is independent of the maximum horizontal stress, unless the fracture is shorter than one borehole radius. For example, Ratigan [18] shows that if the fracture is longer than five borehole radia, the reopening pressure will be equal to the minimum horizontal stress.

Our results indicate that it is only possible to obtain a reopening pressure that is dependent on the maximum horizontal stress, if fracture opening is limited to a distance smaller than one borehole radius and if the well-bore storage is extremely small. In a field situation, it is very difficult to control the fracture growth to less than a borehole radius. When inducing a fracture, the hydraulic line is loaded with several liters of water, which is instantaneously released into the fracture during the unstable fracture propagation. According to theoretical models of hydraulic fracturing, a few liters injection would result in a fracture length of about one meter. Even if the fracture growth can be limited to one borehole radius (38 mm in our case), the reopening of the fracture could probably not be noticed in the well-pressure response. This is because the compliance of such a small fracture is very small compared to the well-bore storage of field test equipment.

A small well storage may be obtained when measurement is performed in a short borehole accessed from a drift. In this case, the fracture growth is better controlled and can be limited. In addition, the fracture may be barely opened during the first pressurization, which implies that fracture shear is minimized and therefore that there is a higher possibility for complete fracture closure. The properties of such a fracture may be different from a tensile fracture produced in a core sample which is completely taken apart. If the fracture in the field closes completely and the normal stiffness is extremely high, the reopening pressure can give a reliable estimate of the maximum horizontal stress.

A reopening test using the sleeve fracturing method [19] can avoid the difficulties with penetrating fracture fluid. In this method, the fracture is initiated and reopened by a pressurization of an inflatable borehole packer. The pressure is applied inside the packer and cannot leak into the rock formation. Therefore, the fracture propagation may be better controlled, keeping the fracture length short. Furthermore, there is no problem with fluid penetrating the fracture, and therefore the fracture opening takes place solely because the borehole wall pressure. With this method, the reopening pressure will still be affected by the stress redistribution presented in Figure 7. However, if the fracture is kept short, the effect of stress redistribution is much smaller than that shown in Figure 7, which is valid for a longer fracture.

Conclusions

The presence of the induced incompletely closed fracture gives the following uncertainties for the determination of the maximum principal horizontal stress using the reopening pressure:

1) Stress is redistributed near the borehole because the fracture is softer than the surrounding rock, which implies that the medium is no longer homogeneously linear elastic. The minimum tangential stress at the borehole wall is therefore different from the theoretical value, assuming a linear elastic medium.
2) During a reopening test, fluid penetrates far into the fracture and opens it by the force of the fluid pressure inside the fracture. Therefore, the near well-bore conditions are less important for the fracture reopening.
3) The fracture opens gradually, and the apparent reopening pressure is caused by a change in system compliance due to the decreasing fracture normal stiffness. The apparent reopening pressure is therefore dependent on the compliance of both the test equipment and the fracture.

The modeling shows that in most practical situations the apparent reopening pressure is similar to the magnitude of the minimum principal horizontal stress, with little or no correlation to the maximum principal horizontal stress. This observation indicates that the estimate of the maximum principal stress from hydraulic fracturing stress measurement using reopening pressure is very uncertain.

Acknowledgments

We gratefully acknowledge the support by Groundwater Protection Division, Office of Ground Water and Drinking Water, U.S. Department of Environmental Protection Agency, under the auspices of the Department of Energy, and the Office of Energy Research, Office of Basic Sciences, through contract number DE-ACOS-79SFD00098.

References

1. Bredehoeft J. D., Wolf R. G., Keys W. S. and Shutter E. Hydraulic fracturing to determine the regional *in situ* stress field in the Piceance Basin, Colorado. *Geol. Soc. Am. Bull***. 87**, 250-258 (1976).
2. Cornet F. H. Interpretation of hydraulic injection test for in-situ stress determination. *Proc. Int. Workshop on Hydraulic Fracturing Stress Measurements* (Zoback and Haimson, Eds), Monterey, pp 149-158. National Academy Press, Washington D.C. (1983).
3. Hardy M. P. and Asgian M. I. Fracture reopening during hydraulic fracturing stress determinations. *Int. J. Rock Mech. Min. Sci. & Geomech. Abstr*. **26**, 489-497 (1989).
4. Rutqvist J., Tsang C.-F. and Stephansson O. Hydraulic field measurements of incompletely closed fractures in granite. *Int. J. Rock mech. Min. Sci. & Geomech. Abstr*. **34,** Paper no. 267 (1997).
5. Iwano, M. (1995). *Hydromechanical Characteristics of a Single Rock Joint.* Ph.D. thesis, Massachusetts Institute of Technology.
6. Rutqvist J. and Stephansson O. Influence of fracture aperture and normal stiffness on the reopening pressure in classical hydraulic fracturing stress measurements. *Proc.*

International symposium on rock stress, Kumamoto, Japan. A. A. Balkema publisher 127-132 (1997).
7. Ito T, Sato A. and Hayashi K. Two methods for hydraulic fracturing stress measurements needless the ambiguous reopening pressure. *Int. J. Rock Mech. Min. Sci. & Geomech. Abstr.* **34**, Paper No. 143 (1997).
8. Noorishad J., Tsang C.-F. and Witherspoon P. A. Theoretical and field studies of coupled behavior of fractured rocks - 1. Development and verification of a numerical simulator. *Int. J. Rock. Mech. Min. Sci. & geomech. Abstr*. **29**, 401-409 (1992).
9. Biot, M. A. General theory of three dimensional consolidation. *J. Applied Physics*, **15**, 155-164 (1941).
10. Goodman, R. E. The mechanical properties of joints. Proc. 3rd Congr. ISRM. Denver, 1A:127-140 (1974).
11. Bandis S., Lunsden A. C. and Barton N. R. Fundamentals of Rock Joint Deformation. *Int. J. Rock Mech. Min. Sci. & geomech. Abstr*. **29**, 249-268 (1983).
12. Witherspoon P. A., Wang J. S. Y., Iwai K. and Gale J. E. Validity of the cubic law for fluid flow in a deformable fracture. *Water Resources Res.* **16**, 1016-1024 (1980).
13. Bjarnasson B., Ljunggren C. and Stephansson O. New development in hydraulic stress measurements at Luleå University of Technology. *Int. J. Rock Mech. Min. Sci. & Geomech. Abstr.* **26**, 579-586 (1989).
14. Cheung L. S. and Haimson B. C. Laboratory study of hydraulic fracturing pressure data–How valid is their conventional interpretaion? *Int. J. Rock Mech. Min. Sci. & Geomech. Abstr.* **26**, 595-604 (1989).
15. Lee M. Y. and Haimson B. C. Statistical evaluation of hydraulic fracturing stress measurement parameters. *Int. J. Rock Mech. Min. Sci. & Geomech. Abstr.* **26**, 447-456 (1989).
16. Morita N., Fuh G.-F. and Black A. D. Borehole breakdown pressure with drilling fluids–II. Semi-analytical solution to predict borehole breakdown pressure. *Int. J. Rock Mech. Min. Sci. & Geomech. Abstr*. **33**, 53-69 (1996).
17. Gou F., Morgenstern N. R. and Scott J. D. Interpretation of hydraulic fracturing breakdown pressure. *Int. J. Rock Mech. Min. Sci. & Geomech. Abstr.* **30**, 617-626 (1993).
18. Ratigan J. L. The use of fracture reopening pressure in hydraulic fracturing stress measurements. *Rock Mech. Rock Engng.* **25**, 225-236 (1992).
19. Ljunggren C. and Stephansson O. Sleeve fracturing–A borehole technique for in-situ determination of rock deformability and rock stresses. *Proc. Int. Symp. on Rock Stress and Rock Stress Measurements* (O. Stephansson Ed). Centek, Stockholm, Sweden (1996).

Figure Captions

Figure 1. Setup of hydraulic fracturing stress measurements in deep boreholes.

Figure 2. The principle of the classical hydraulic fracturing stress measurement technique with the first and second pressurization cycles. Well-pressure and pump-injection flow is presented as a function of time, and the borehole and fracture is illustrated in horizontal sections.

Figure 3. Uncertainties due to the initial hydraulic aperture of the induced fracture.

Figure 4. Finite element model of a horizontal section through a vertical borehole and a vertical fracture.

Figure 5. Mechanical aperture versus effective normal stress for Goodman's and Bandis' models.

Figure 6. Tangential stress as a result of modeling a) without fracture and b) with fracture. The remote stresses are isotropic at 10 MPa, and the fluid pressure is zero.

Figure 7. Minimum principal horizontal stress for different horizontal stress factors (σ_H/σ_h) versus tangential wall stress concentration factor ($\sigma_{\theta min}/\sigma_h$).

Figure 8. Well-pressure and flow rate into the fracture during injection at moderate remote stress. The minimum horizontal stress is 10 MPa, and the maximum horizontal stress is 10 (solid line) and 30 MPa (dashed line). Pump-injection rate is 6 liters/minute.

Figure 9. Fluid pressure, half fracture hydraulic aperture and effective normal stress during injection at moderate remote stress. The minimum horizontal stress is 10 MPa, and the maximum stress is 10 (solid line) and 30 MPa (dashed line).

Figure 10. Well-pressure and flow rate into the fracture during injection at high remote stress. The minimum horizontal stress is 50 MPa, and the maximum horizontal stress is 50 (solid line) and 150 MPa (dashed line). Pump-injection rate is 40 liters/minute.

Figure 11. Fluid pressure, half fracture hydraulic aperture and effective normal stress during injection at high remote stress. The minimum horizontal stress is 50 MPa, and the maximum stress is 50 (solid line) and 150 MPa (dashed line).

Figure 12. Well-pressure and flow rate into the fracture during injection at high remote stress and a very low well storage. The minimum horizontal stress is 50 MPa, and the maximum horizontal stress is 50 (solid line) and 150 MPa (dashed line). Pump-injection rate is 0.1 liters/minute.

Figure 13. Fluid pressure, half fracture hydraulic aperture and effective normal stress during injection at high remote stress and with a very low well storage. The minimum

horizontal stress is 50 MPa, and the maximum stress is 50 (solid line) and 150 MPa (dashed line).

Table 1. Material parameters for modeling of fracture reopening tests on an induced fracture in granitic rocks

Material	Parameter	Value
Fluid	Mass density, ρ_f	1000 kg/m^3
	Compressibility, C_f	4.4x10^{-10} Pa^{-1}
	Dynamic viscosity, μ_f	1x10^{-3} Ns/m^2
Rock matrix	Young's modulus, E_r	60 GPa
	Poisson's ratio, ν_r	0.25
	Mass density, ρ_r	2700 kg/m^3
	Permeability, k	1x10^{-19} m^2
	Biot's constant, α_r	1.0
	Biot's constant, M_r	130 Gpa
Fracture	Joint constant, A_i	62.5
	Joint constant, σ'_{n0}	0.625 MPa
	Res. Hydraulic aperture, b_{hr}	0
	Factor, f	0.5
	Normal stiffness*, k_{n5}	500 GPa/m
	Hydraulic aperture*, b_{h5}	11 μm
	Biot's constant, α	1.0
	Biot's constant, M	2.27 GPa
	Length, l	1 m

*At 5 MPa effective normal stress

Table 2. Summary of apparent reopening pressure as a result of modeling and comparison to reopening pressure predicted by Equations (1), (3) and (4) for the given remote stress.

Minimum horizontal Stress, σ_h (MPa)	Maximum horizontal Stress, σ_H (MPa)	Well-bore storage	Reopening pressure (MPa)				
			Modeling	Eq. (1)	Eq. (1) $P_0 = 0$	Eq. (3)	Eq. (4)
10	10	High	11	15	20	10*	10*
10	30	High	11	-5	0	0	10*
50	50	High	62	80	100	50*	50*
50	150	High	60	-20	0	0	50*
50	50	Very low	40	80	100	50*	50*
50	150	Very low	30	-20	0	0	50*

*The best prediction of the modeling results.

Figure 1

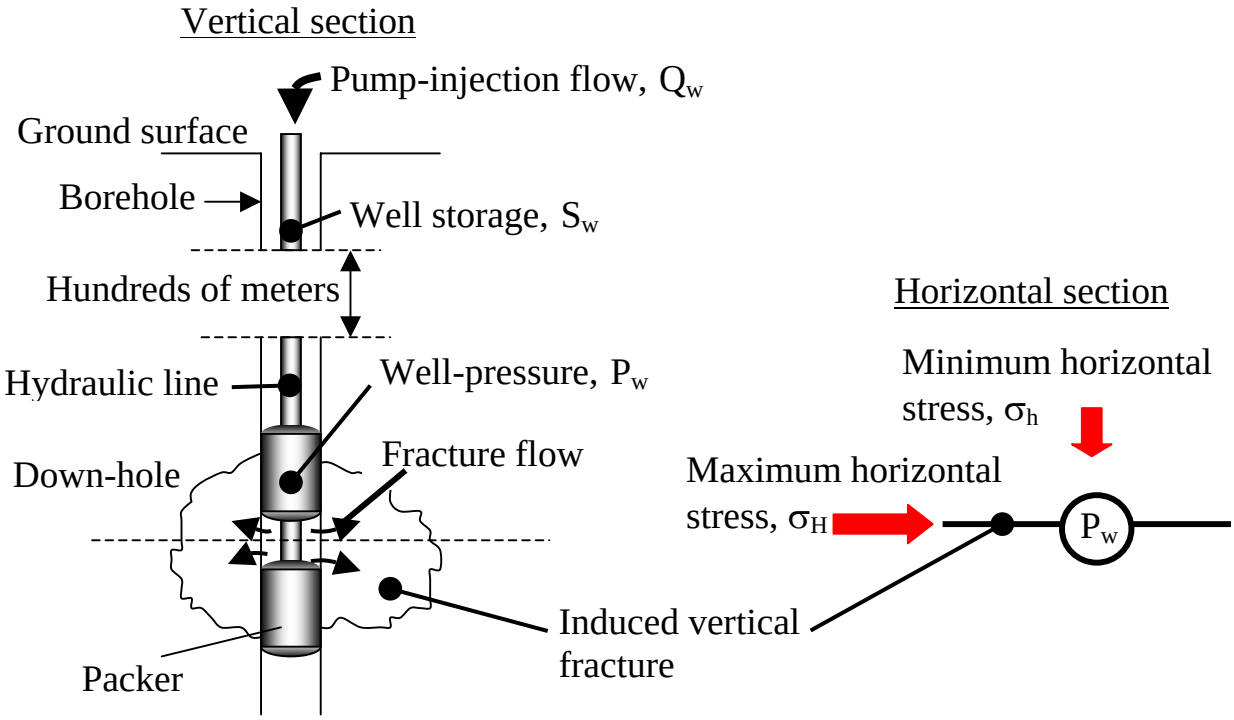
Vertical section
Pump-injection flow, Q_w
Ground surface
Borehole
Well storage, S_w
Hundreds of meters
Hydraulic line
Well-pressure, P_w
Down-hole
Fracture flow
Packer
Induced vertical fracture
Horizontal section
Minimum horizontal stress, σ_h
Maximum horizontal stress, σ_H
P_w

Figure 2

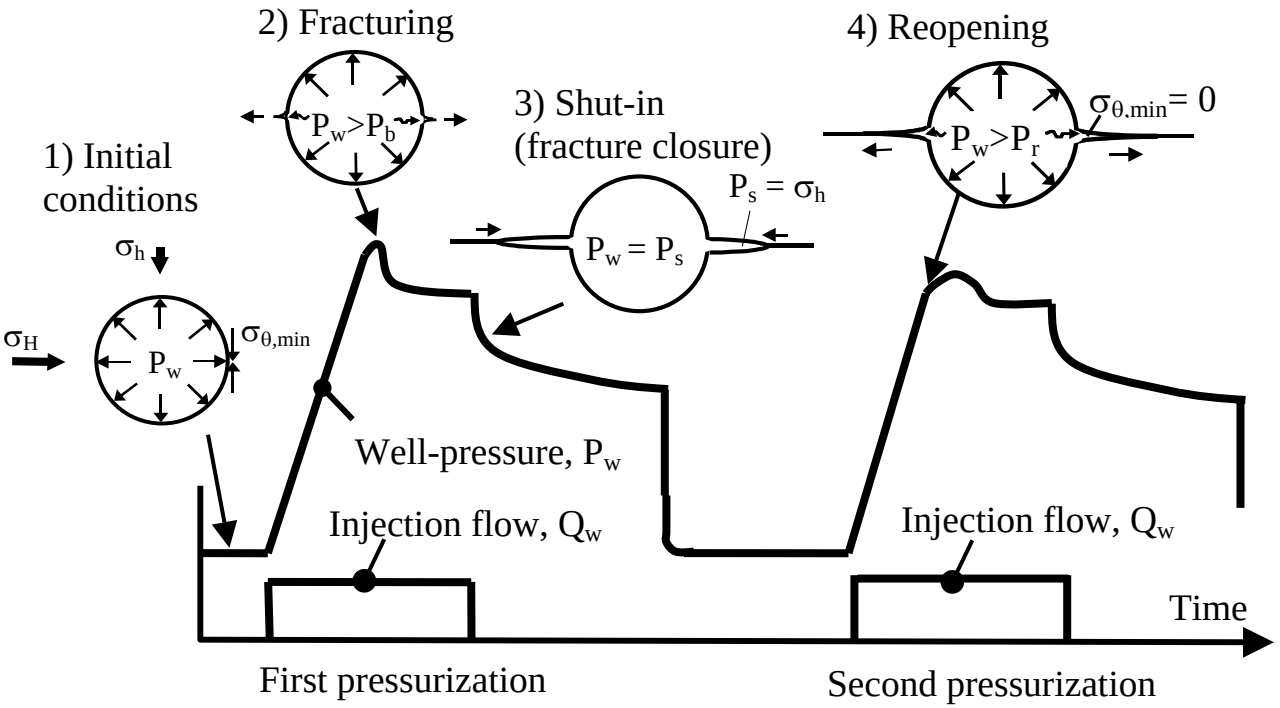
2) Fracturing
4) Reopening
3) Shut-in
(fracture closure)
1) Initial
conditions
$P_w > P_b$
$P_w > P_r$
$\sigma_{\theta,min} = 0$
$P_s = \sigma_h$
$P_w = P_s$
σ_h
σ_H
P_w
$\sigma_{\theta,min}$
Well-pressure, P_w
Injection flow, Q_w
Injection flow, Q_w
Time
First pressurization
Second pressurization

Figure 3

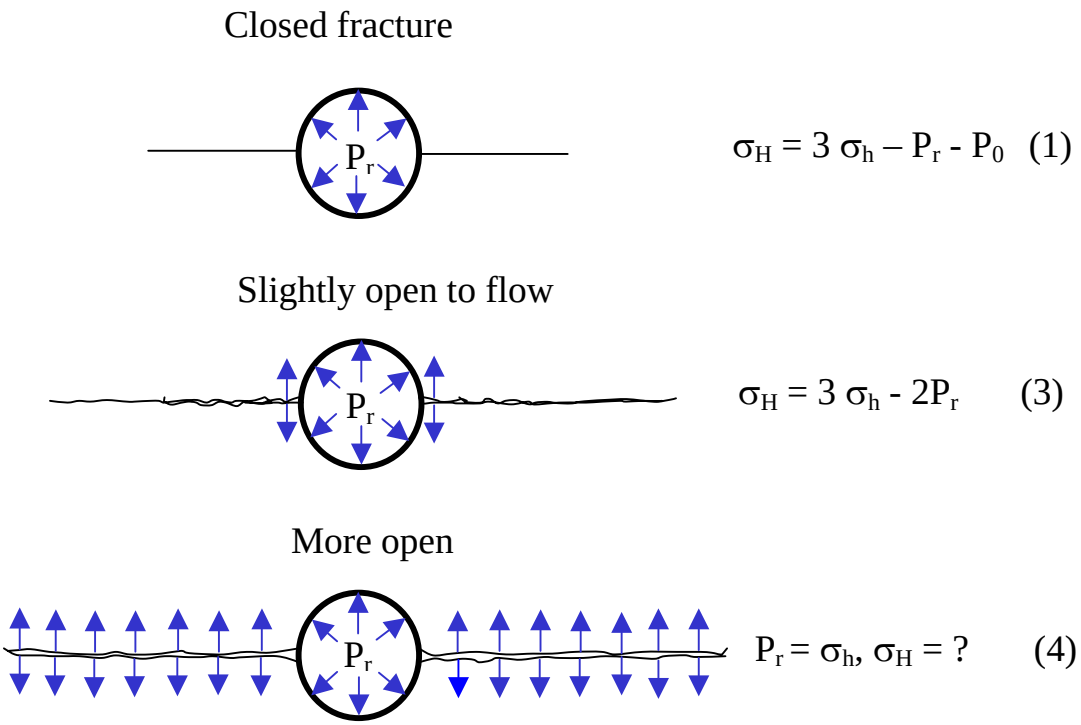
Closed fracture
P_r
$\sigma_H = 3\,\sigma_h - P_r - P_0$ (1)
Slightly open to flow
P_r
$\sigma_H = 3\,\sigma_h - 2P_r$ (3)
More open
P_r
$P_r = \sigma_h$, σ_H = ? (4)

Figure 4

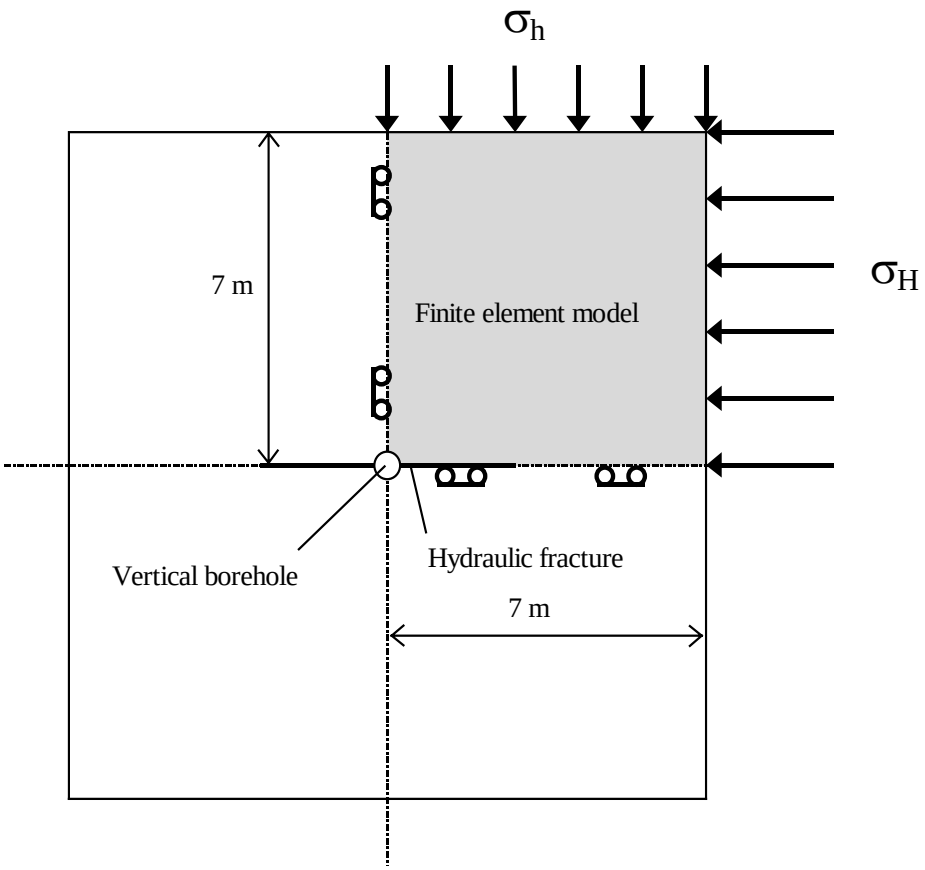
σh
σH
7 m
Finite element model
Vertical borehole
Hydraulic fracture
7 m

Figure 5

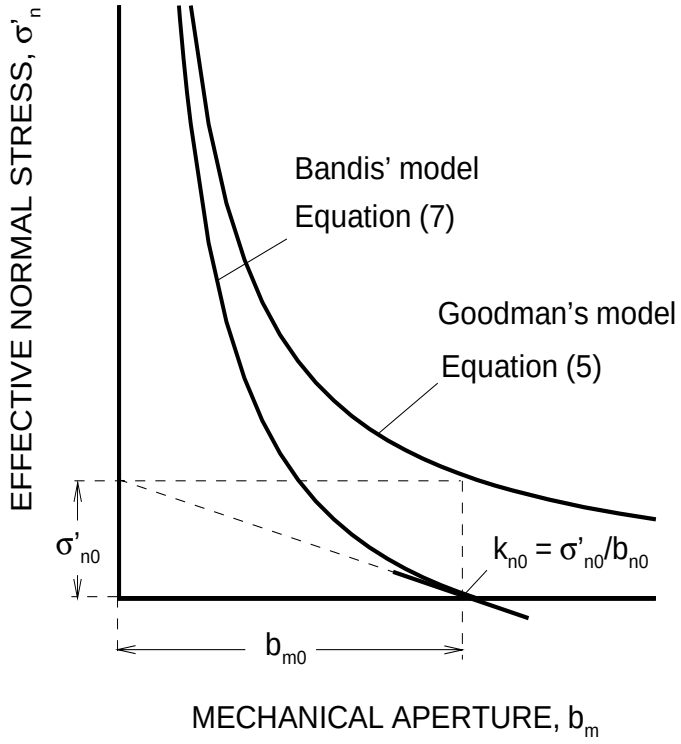
EFFECTIVE NORMAL STRESS, σ'n
Bandis' model
Equation (7)
Goodman's model
Equation (5)
σ'n0
kn0 = σ'n0/bn0
bm0
MECHANICAL APERTURE, bm

Figure 6

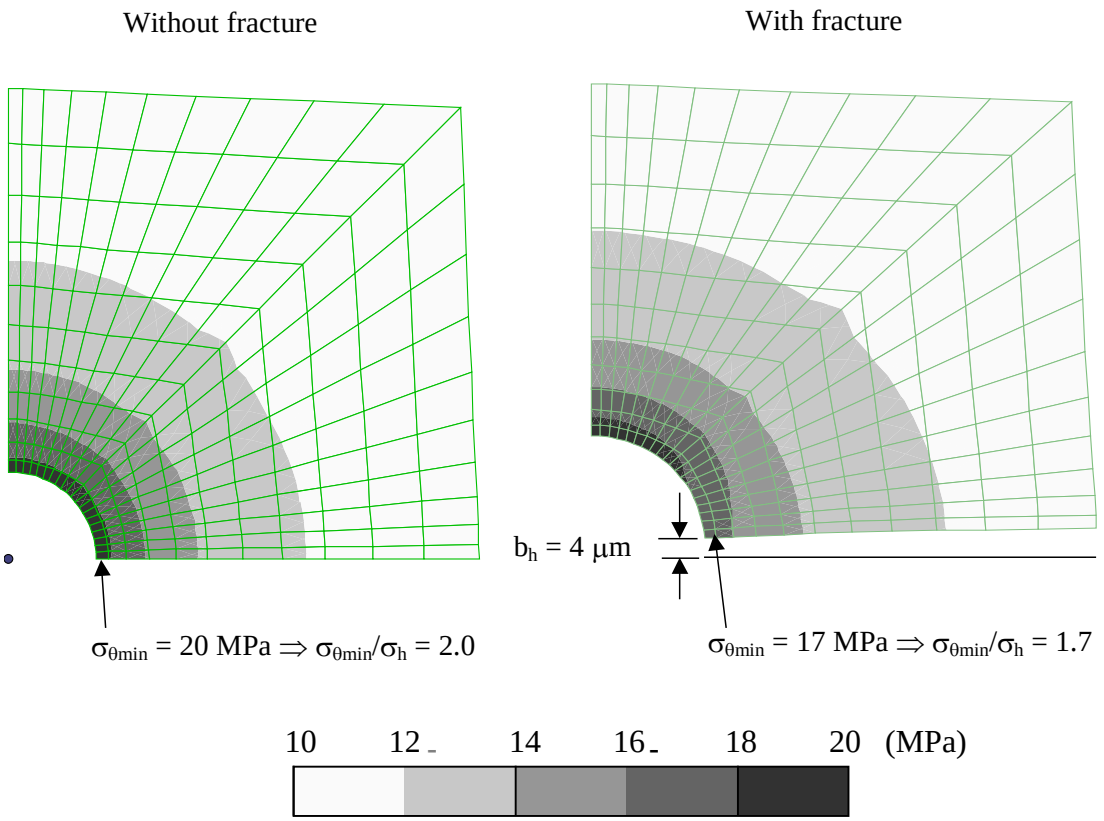
Without fracture
With fracture
b_h = 4 μm
$\sigma_{\theta min}$ = 20 MPa ⇒ $\sigma_{\theta min}/\sigma_h$ = 2.0
$\sigma_{\theta min}$ = 17 MPa ⇒ $\sigma_{\theta min}/\sigma_h$ = 1.7
10
12
14
16
18
20
(MPa)

Figure 7

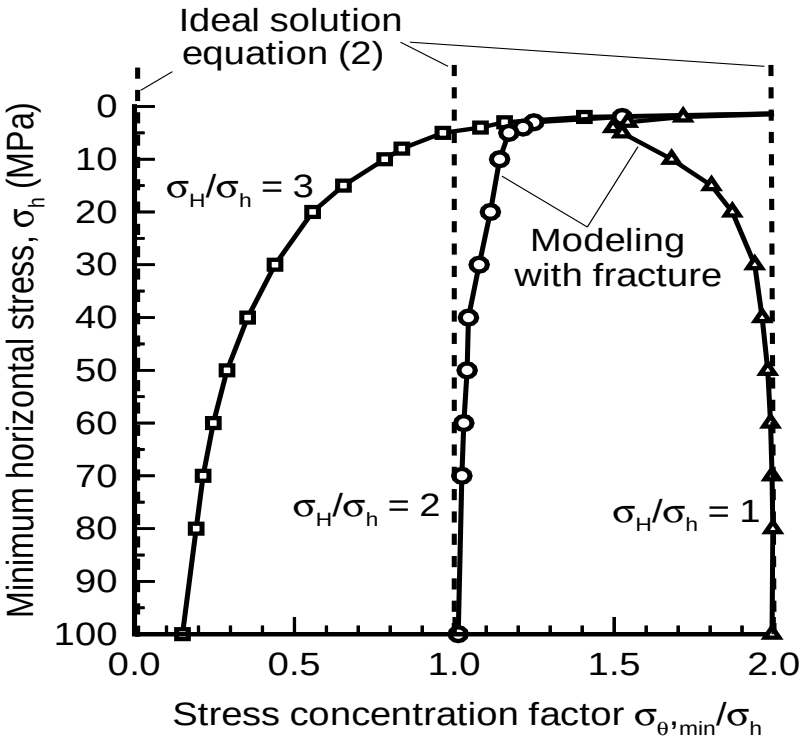
Ideal solution
equation (2)
Modeling
with fracture
σH/σh = 3
σH/σh = 2
σH/σh = 1
Minimum horizontal stress, σh (MPa)
0
10
20
30
40
50
60
70
80
90
100
0.0
0.5
1.0
1.5
2.0
Stress concentration factor σθ,min/σh

Figure 8

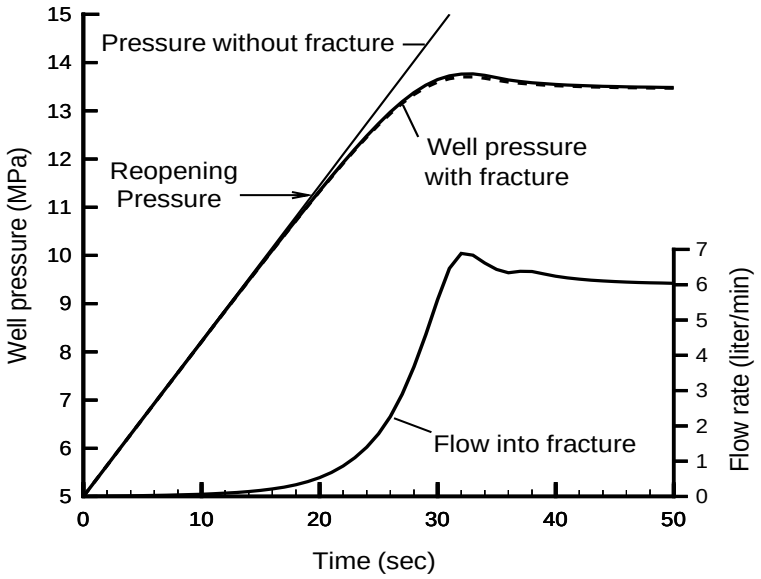
Pressure without fracture
Well pressure
with fracture
Reopening
Pressure
Flow into fracture
Well pressure (MPa)
Flow rate (liter/min)
Time (sec)
15
14
13
12
11
10
9
8
7
6
5
7
6
5
4
3
2
1
0
0
10
20
30
40
50

Figure 9

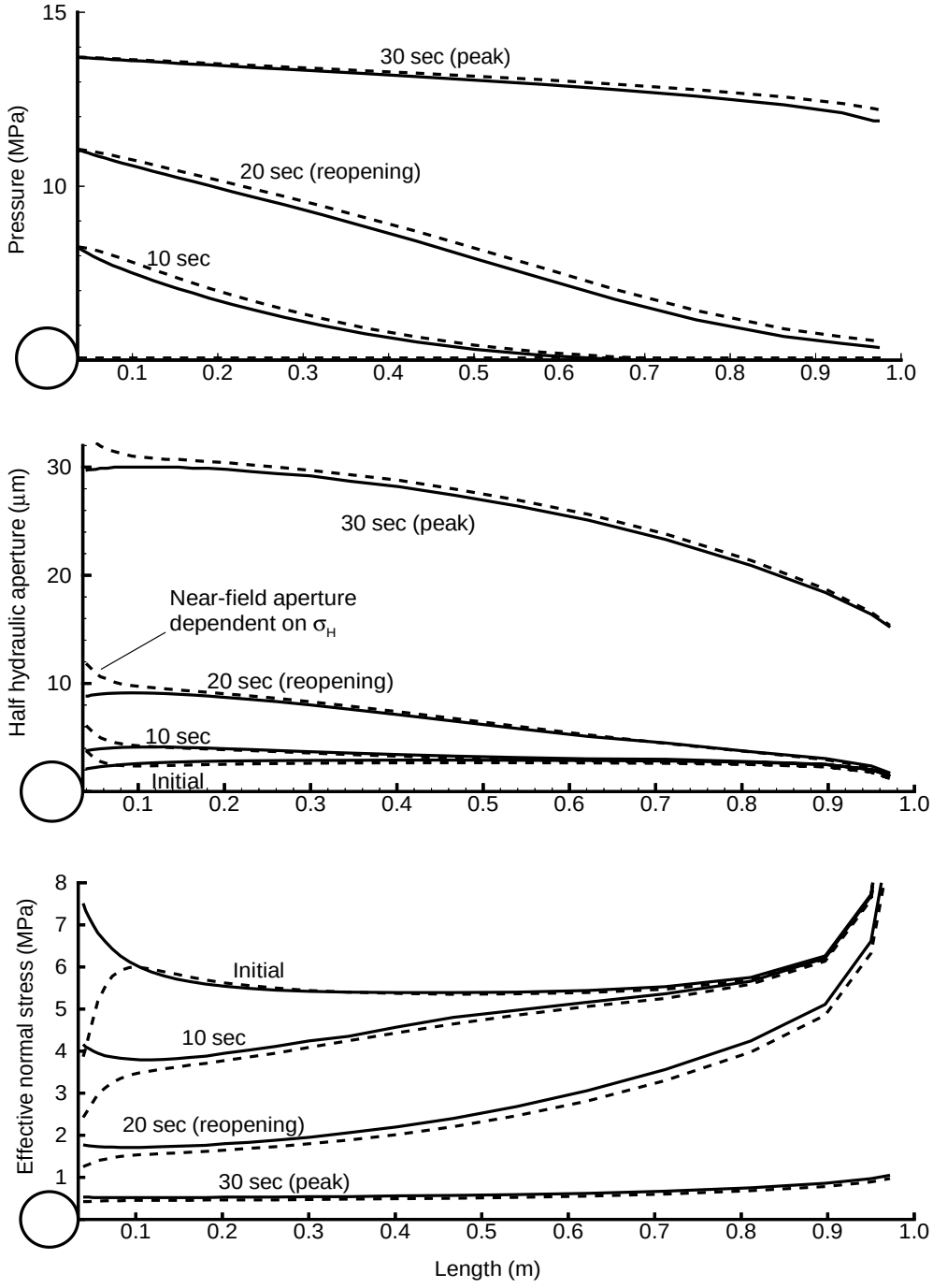
Pressure (MPa)
15
10
30 sec (peak)
20 sec (reopening)
10 sec
0.1
0.2
0.3
0.4
0.5
0.6
0.7
0.8
0.9
1.0
Half hydraulic aperture (μm)
30
20
10
30 sec (peak)
Near-field aperture
dependent on σ_H
20 sec (reopening)
10 sec
Initial
Effective normal stress (MPa)
8
7
6
5
4
3
2
1
Initial
10 sec
20 sec (reopening)
30 sec (peak)
Length (m)

Figure 10

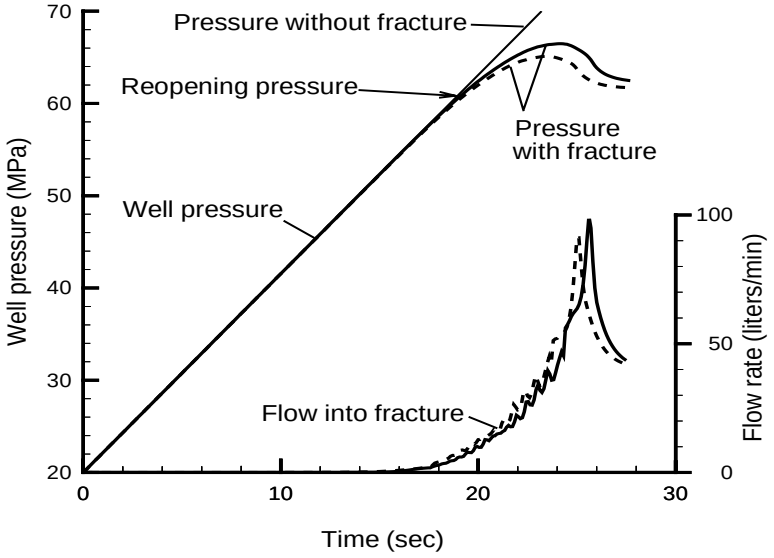
Pressure without fracture
Reopening pressure
Pressure
with fracture
Well pressure
Flow into fracture
Well pressure (MPa)
Flow rate (liters/min)
Time (sec)
70
60
50
40
30
20
100
50
0
0
10
20
30

Figure 11

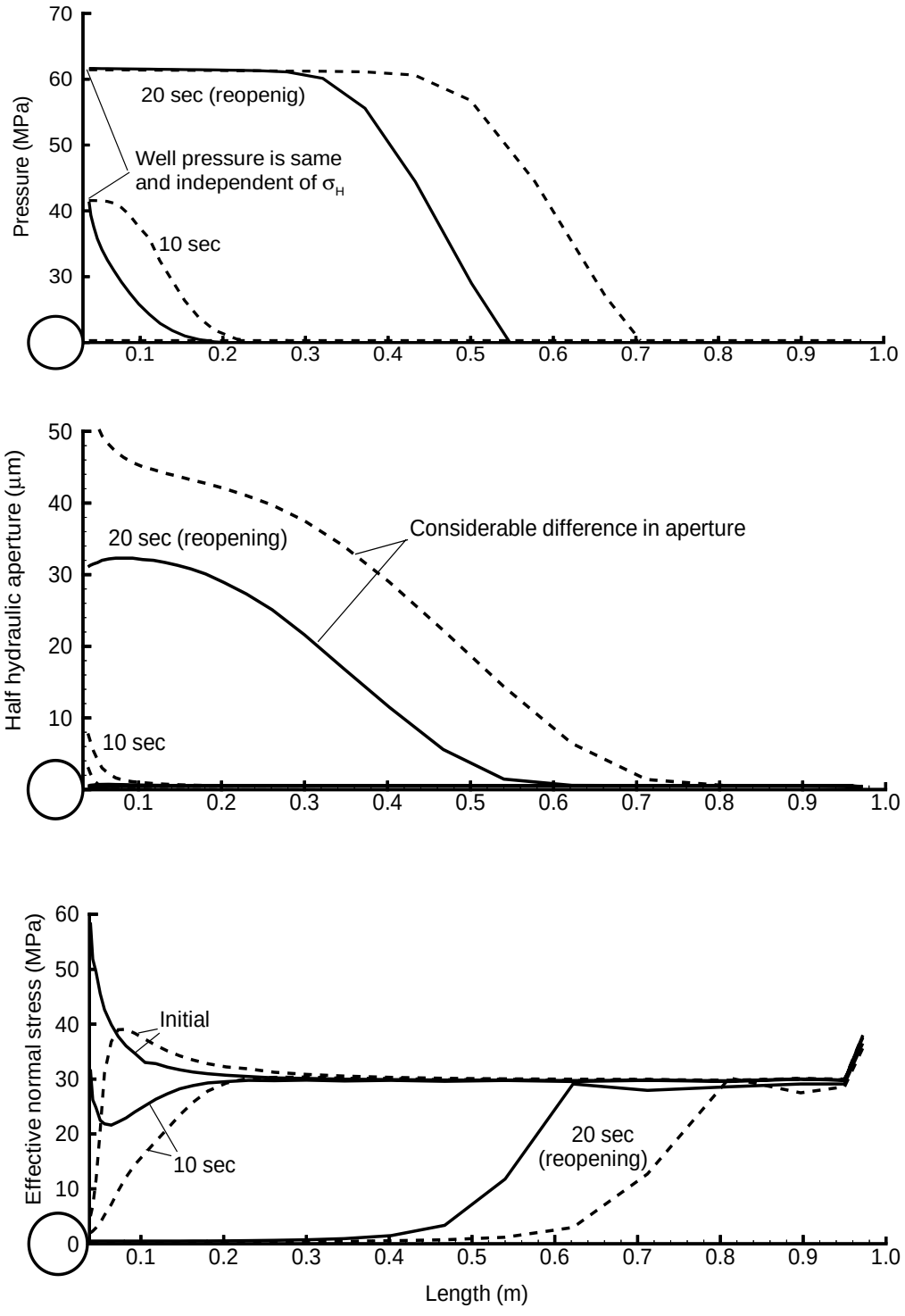
Pressure (MPa)
70
60
50
40
30
20 sec (reopenig)
Well pressure is same
and independent of σ_H
10 sec
0.1
0.2
0.3
0.4
0.5
0.6
0.7
0.8
0.9
1.0
Half hydraulic aperture (μm)
50
40
30
20
10
20 sec (reopening)
Considerable difference in aperture
10 sec
Effective normal stress (MPa)
60
50
40
30
20
10
0
Initial
10 sec
20 sec
(reopening)
Length (m)

Figure 12

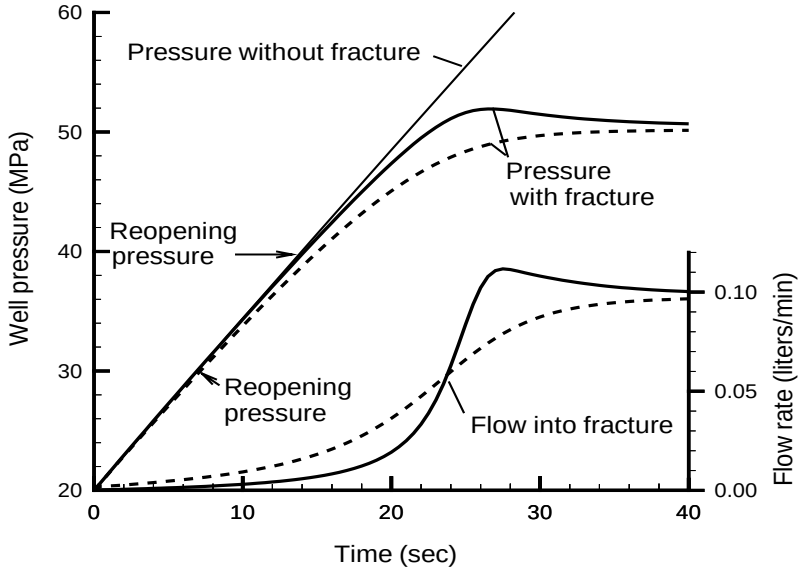
Pressure without fracture
Pressure
with fracture
Reopening
pressure
Reopening
pressure
Flow into fracture
Well pressure (MPa)
Flow rate (liters/min)
Time (sec)
60
50
40
30
20
0
10
20
30
40
0.10
0.05
0.00

Figure 13

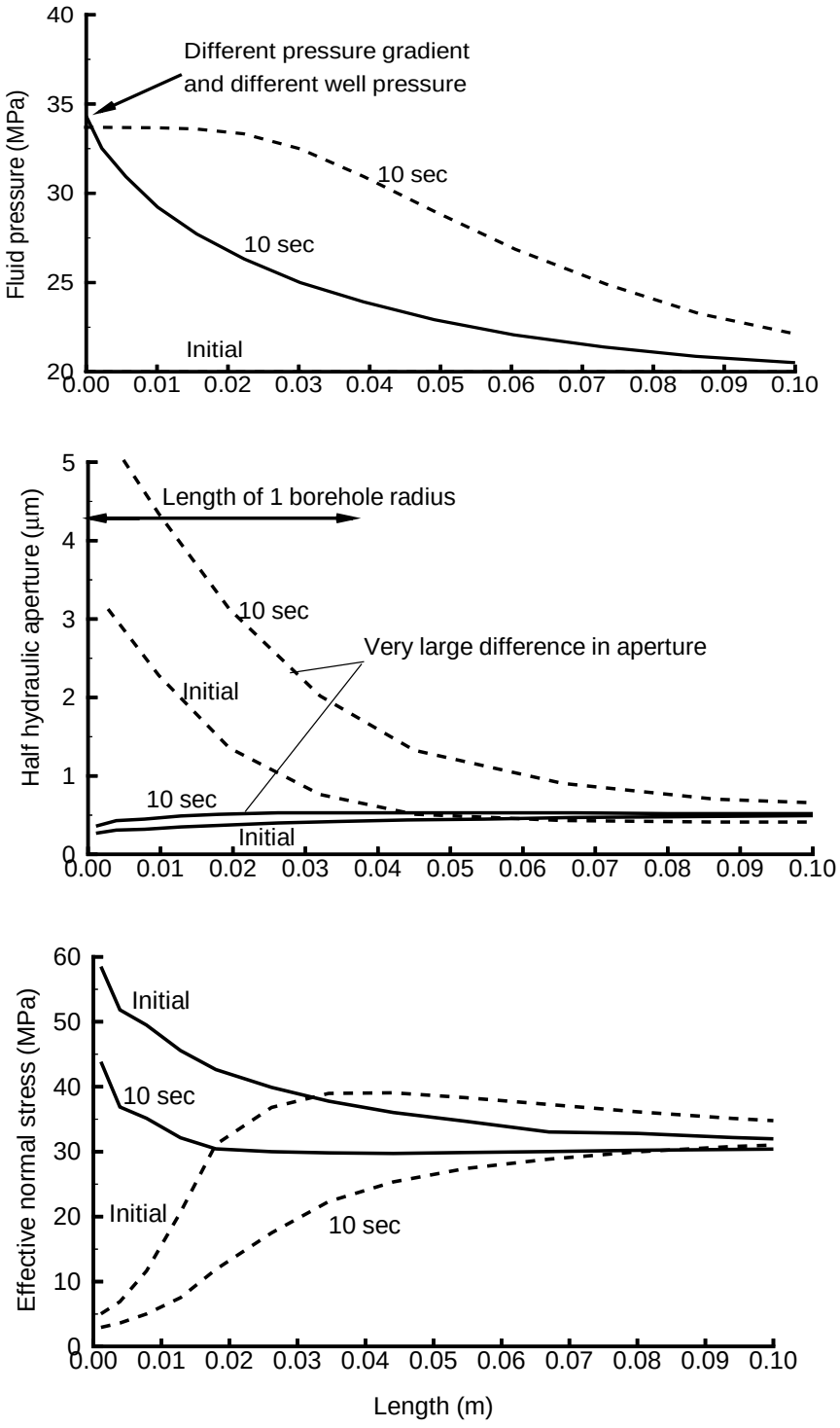
Fluid pressure (MPa)
Different pressure gradient
and different well pressure
10 sec
10 sec
Initial
Half hydraulic aperture (μm)
Length of 1 borehole radius
10 sec
Very large difference in aperture
Initial
10 sec
Initial
Effective normal stress (MPa)
Initial
10 sec
Initial
10 sec
Length (m)